

Bayesian Reasoning for Physics Informed Neural Networks

Krzysztof M. Graczyk¹ and Kornel Witkowski²

¹Institute of Theoretical Physics,
University of Wrocław,

pl. M. Borna 9, 50-204 Wrocław, Poland

²Institute of Low Temperature and Structure Research,
Polish Academy of Sciences,
ul. Okólna 2, Wrocław, 50-422, Poland

April 30, 2024

Abstract

We present the application of the physics-informed neural network (PINN) approach in Bayesian formulation. We have adopted the Bayesian neural network framework to obtain posterior densities from Laplace approximation. For each model or fit, the evidence is computed, which is a measure that classifies the hypothesis. The optimal solution is the one with the highest value of evidence. We have proposed a modification of the Bayesian algorithm to obtain hyperparameters of the model. We have shown that within the Bayesian framework, one can obtain the relative weights between the boundary and equation contributions to the total loss. Presented method leads to predictions comparable to those obtained by sampling from the posterior distribution within the Hybrid Monte Carlo algorithm (HMC). We have solved heat, wave, and Burger's equations, and the results obtained are in agreement with the exact solutions, demonstrating the effectiveness of our approach. In Burger's equation problem, we have demonstrated that the framework can combine information from differential equations and potential measurements. All solutions are provided with uncertainties (induced by the model's parameter dependence) computed within the Bayesian framework.

1 Introduction

The deep learning (DL) revolution impacts almost every branch of life and sciences [1]. The deep learning models are also adapted and developed for solving problems in physics [2]. The statistical analysis of the data is one of the popular and straightforward domains of application of neural networks in physics [3, 4]. Another one is using DL-like models to optimize and modernize computational systems in physics, starting from solvers for fluid flow [5, 6] and finishing on the Monte Carlo generators in particle physics [7]. Deep neural networks are examples of artificial neural networks (NNs) studied and utilized in various branches of life and science for years [8]. In this paper, we consider the feed-forward shallow neural networks, with one or maximally two layers of hidden units, that are utilized to solve partial differential equations (PDEs).

Differential equations are the essence of physics. Indeed, they describe the system and its evolution in time in classical mechanics, electrodynamics, fluid physics, quantum mechanics, Etc. Some can be solved analytically, but a vast class of problems can be solved numerically only.

One of the exciting ideas is to adapt a neural network framework to solve PDEs numerically. The problem of numerical integration comes down to the optimization problem. Indeed, the approximate solution of a differential equation is parametrized by a feed-forward neural network that depends on the parameters (weights). The optimal solution minimizes a cost function defined for a given equation. One of the first successful formulations of this idea was provided by Lagaris et al. [9]. They applied the method to ordinary and partial differential equations. It was assumed that the feed-forward neural network, modified to satisfy initial or boundary conditions, was a solution of an equation. A similar idea was exploited by Lagaris *et al.* for solving eigenvalue problems in quantum mechanics [10].

One of the problems of the Lagaris *et al.* approach was its relatively low universality, i.e., for each differential equation, one has to encode the initial or boundary conditions in the network parametrization. Although the final solution exactly satisfies the required requirements, the training of such a network could be smoother. Therefore, in modern applications, the boundary or initial conditions are introduced as additional contributions to the cost function. As a result, the boundary or initial constraints are satisfied by the obtained solution only on an approximate level. However, the optimization goes much smoother than in the Lagaris *et al.* approach. This new approach was formulated by Raissi *et al.* [11, 12, 13] and called *Physics Informed Neural Network* (PINN). Two classes of problems were discussed: data-driven solutions and data-driven discovery of PDEs. The PINN method has been popular, and it has been exploited for forward and inverse types of the problems [14, 15, 15, 16, 17, 18, 19, 20, 21, 22, 23]. An extensive literature review on PINNs is given by Cuomo *et al.* [24].

Karniadakis *et al.* [25] provides a comprehensive review of the PINN approach. In particular, they point out the major difficulties of the approach, namely, the problem of tuning the hyperparameters, fixing relative weights between various terms in the loss function, and the convergence to the global minimum. The PINN idea can be naturally extended to a broader class of problems than PDEs, in which the neural networks or machine learning systems are adapted to solve the problem or to optimize the system that solves the problem, see reviews by Faroughi *et al.* [26] (the physics guided, informed, and encoded neural network approaches), Meng *et al.* [27] and Hao *et al.* [28] (physics informed machine learning including PINNs).

Artificial neural networks have been studied for more than sixty years [29, 30, 31, 8]. Before the deep learning revolution, shallow feed-forward neural networks had been extensively studied. Algorithms for treatments of the networks have been developed. However, many of the achievements for shallow networks do not apply to deep neural networks because of the complexity of the DL systems. Nevertheless, even for the small NNs, there were several difficulties that one had to face, namely, overfitting problem, choice of the proper network architecture and model hyperparameters, and estimation of the uncertainties in network predictions. Bayesian statistics offer systematic methods that allow one to overcome these difficulties. Hence, in the nineties of the XX century, the Bayesian methods were discussed and adapted for artificial neural networks [32].

Usually, in data analysis, the methods of frequentistic rather than Bayesian statistics are utilized. There are essential differences between both methodologies [33]. The Bayesian approach seems to be more subjective in the formulation than frequentistic. However, the way the Bayesian framework (BF) is defined allows a user to control the subjectivity of assumptions. From that perspective, Bayesian statistics can be used to study the impact of the model assumptions on the analysis results[34].

In Bayesian statistics, one must evaluate the posterior probabilities. The probability is a measure of the degree of belief that an event will occur [33]. The initial (prior assumptions) are encoded in the prior probabilities. Bayes' rule is used to obtain the posterior probabilities. Note that the posterior probability can continuously be updated when new data or information arrives. Moreover, within the BF, it is possible to consider various types of uncertainties [35], namely, uncertainty due to the noise of the data (aleatoric), the lack of knowledge of the model parameters, and model-dependence of the assumptions (epistemic).

Ultimately, it is possible to quantitatively and, in some sense, objectively compare various models and choose the one that is the most favorable to the data. Eventually, BF embodies Occam's razor principle [34, 36]. The models that are too complex (with too many parameters, in the case of a neural network with too many units) are naturally penalized. Hence, the models obtained in the BF should not tend to overfit the data.

When the PDEs are solved with the PINN method, initial or boundary conditions can be naturally understood as prior assumptions. Moreover, the BF allows one to infer from the data the parameters that parameterize PDEs or directly the form of the PDEs. Eventually, the Bayesian PINN solution is provided with uncertainties. Therefore the Bayesian approach to the PINN is one of the directions explored in the last years [37].

Indeed, there are many papers where various algorithmic formulations of the Bayesian PINNs are given [38, 39, 40]. The initial works concerned adapting the Gaussian process technique [41] for regression [42, 43] – the infinitely wide one-hidden layer network can be understood as a Gaussian process [44]. In many applications to obtain the posterior distributions, the Hamiltonian Monte Carlo and the variational inference are adapted [45, 46, 47, 48]. The broad class of Bayesian algorithms

utilized for training neural networks is discussed in a survey by Magris and Iosifidis [49].

In the present paper, we propose to adapt the Bayesian framework (BF) for neural networks [50, 51, 52] whose works were motivated by results of Gull [36, 53] and Skilling [54]. A pedagogical review of the approach is given by Bishop in Ref. [32].

In the BF, all necessary probabilities are expressed in the Gaussian form. Indeed, the Laplace approximation is imposed to evaluate the posterior distribution. As a result, all probability densities are obtained in analytic form. The so-called evidence is estimated - a measure that classifies the models. The framework allows us to choose the most optimal network architecture for a given problem objectively, compare distinct network models, estimate the uncertainties for the network predictions and the network weights, and fine-tune the model’s hyperparameters. In the past, we have adapted MacKay’s framework to study the electroweak structure of the nucleons [55, 56, 57, 4, 58, 3]. For that project we developed our own C++ Bayesian neural network library. In contrast, in the present project, we utilize PyTorch environment [59].

In this paper, we show that with BF adapted for PINNs, one can numerically solve PDFs such as heat, wave, and Burger’s equations. We propose some modifications to the original BF’s algorithm. Namely, we improved the procedure that updates the hyperparameters. Additionally, the Bayesian framework allowed us to fine-tune the models’ hyperparameters, including the loss components’ relative weights. As a result, the presented method fine-tunes the impact of the boundary terms on the solution. It is a different approach than approaches proposed in the previous investigations. Typically, the relative weights are tuned based on experimental pre-runs of the model [60] or adapted to the particular type of problem. There are also proposed techniques that allow one to tune the hyperparameters in the optimization process, see Refs. [61, 62, 63, 64]. As mentioned above, this paper proposes a different approach based on the Bayesian reasoning arguments.

The paper is organized as follows: after the introduction in Sect. 2 we describe shortly PINNs. The BF is reviewed in Sec. 3. In Sec. 4, we show the comparison of HMC and this paper Bayesian framework to nonlinear regression problem (Sec. 4.1), additionally we present the solutions of heat (Sec. 4.2), wave (Sec. 4.3), and Burger’s (Sec. 4.4) equations. In Sec. 5, we summarize.

2 PINN

2.1 Multilayer perceptron configuration

We shall consider the feed-forward neural network in the multilayer perceptron (MLP) configuration. The MLP, denoted by \mathcal{N} , represents a nonlinear map from the input space of the dimension d_{in} to the output space of the dimension d_{out} ,

$$\mathcal{N} : \mathbb{R}^{d_{in}} \mapsto \mathbb{R}^{d_{out}}. \tag{1}$$

Note that $\mathcal{N} = \mathcal{N}(\mathbf{x}, \mathbf{w})$ is a function of input vector $\mathbf{x} \in \mathbb{R}^{d_{in}}$ and its parameters called weights, denoted by the vector $\mathbf{w} = (w_1, \dots, w_i, \dots, w_W)$, where W is the total number of weights in a given network.

The MLP is represented by a graph consisting of several layers of connected units (nodes). Each edge of the graph corresponds to a function parameter, a weight, w_i . A unit (node) in a given layer is a single-valued function (activation function). Note that every unit, except the bias unit, is connected with the nodes from the previous layer. In a graph representing a neural network, we distinguish an input (input units), hidden layers of units, and an output layer. Each layer (except the output layer) has a bias unit connected only with the following layer units. It is a single-valued constant function equal to one. An example of a graph of a network with three-dimensional input and two-dimensional output is given in Fig. 1. This network has two hidden layers with five and three hidden units. The properties of the network, \mathcal{N} , are determined by its structure (architecture – topology of the connections) and the type of activation functions that settle in the neurons (units).

The universal approximation theorem [65, 66, 67] states that a feed-forward neural network with at least one layer of hidden units can approximate well any given continuous function. It is a fundamental property of neural networks used extensively in nonlinear regression and classification problems.

Note that the increasing number of units in the neural network broadens its adaptive abilities. However, if a network is large (contains many hidden units), then there is a danger that it can overfit the data, and as a result, it has low generalization abilities. On the other hand, if the network is small (low number of hidden units), it tends to underfit the data. This dilemma is known as the bias-variance

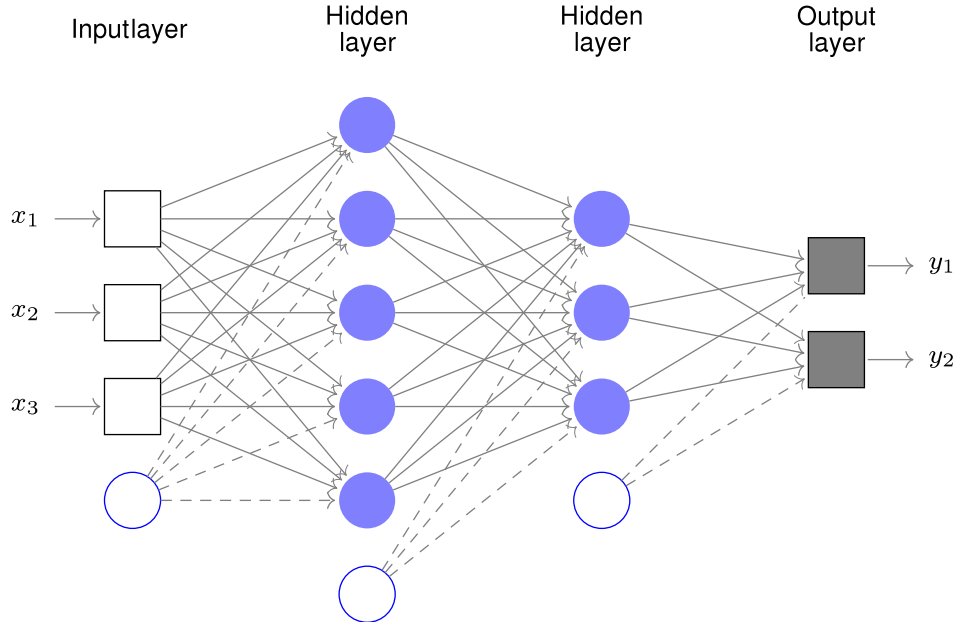


Figure 1: The above MLP contains two hidden unit layers. Empty squares denote the input, whereas filled circles represent the output; Blue filled and open circles indicate hidden and bias units, respectively.

trade-off [68]. There are some rules of thumb on how to solve the problem of under/over-fitting. The most popular is to constrain the values of the weight parameters by adding to the loss (6) the penalty term of the form:

$$E_w = \frac{\alpha}{2} \sum_{i=1}^W w_i^2, \quad (2)$$

where α is the decay width parameter. There are other popular methods. However, we shall utilize the one described above because of its Bayesian interpretation. Note that we shall consider several decay width parameters accommodated in the vector $\boldsymbol{\alpha}$ below.

2.2 PINN: a formulation

We formulate the PINN approach similarly as in Ref. [60]. Let us consider the sets of equations:

$$Eq_i(\mathbf{x}, \hat{f}, \partial\hat{f}, \partial\partial\hat{f}) = 0, \quad i = 1, 2, \dots, q, \quad \mathbf{x} \in \mathcal{M}, \quad (3)$$

$$\mathcal{B}_j(\mathbf{x}, \hat{f}, \partial\hat{f}) = 0, \quad j = 1, 2, \dots, b, \quad \mathbf{x} \in \partial\mathcal{M}, \quad (4)$$

where Eq_i 's and \mathcal{B}_j 's are the differential and boundary operators respectively; $\mathcal{M} \subseteq \mathbb{R}^d$, $d = 1, 2, \dots$; \hat{f} is the solution of the equations (3)-(4). Note that $\partial\hat{f}$ and $\partial\partial\hat{f}$ refer to any first-order partial derivative and second-order derivatives with respect to the input variables, respectively.

In the simplest version of the PINN approach, it is assumed that an approximate solution of the (3) with boundary conditions (4) is given by neural network $\mathcal{N}(\mathbf{x}; \mathbf{w})$. Then, the network solution, $\mathcal{N}(\mathbf{x}; \mathbf{w}^*)$ is so that

$$\mathbf{w}^* = \arg \min_{\mathbf{w}} E, \quad (5)$$

where

$$E = \frac{1}{2} \sum_{i=1}^q \beta_q^i \sum_{k=1}^{N_q} [Eq_i(\mathbf{x}_k; \mathcal{N}(\mathbf{x}_k, \mathbf{w}), \partial\mathcal{N}(\mathbf{x}_k, \mathbf{w}), \partial\partial\mathcal{N}(\mathbf{x}_k, \mathbf{w}))]^2 + \frac{1}{2} \sum_{j=1}^b \beta_b^j \sum_{k=1}^{N_b} [\mathcal{B}_j(\mathbf{x}_k; \mathcal{N}(\mathbf{x}_k, \mathbf{w}), \partial\mathcal{N}(\mathbf{x}_k, \mathbf{w}), \partial\partial\mathcal{N}(\mathbf{x}_k, \mathbf{w}))]^2. \quad (6)$$

The parameters β_q^i 's and β_b^j 's control the relative weights of the components of the loss E . To simplify the discussion, we shall consider only one $\beta_q^i = \beta_q$ and one $\beta_b^j = \beta_b$. We keep them together in the vector $\boldsymbol{\beta} = (\beta_q, \beta_b)$. Moreover, in this paper, we consider the PDEs with $q = 1$. Hence, the loss consists of

$$E_D^q = \frac{1}{2} \sum_{k=1}^{N_q} (E_q(\mathbf{x}_k; \mathcal{N}(\mathbf{x}_k, \mathbf{w}), \partial\mathcal{N}(\mathbf{x}_k, \mathbf{w}), \partial\partial\mathcal{N}(\mathbf{x}_k, \mathbf{w})))^2 \quad (7)$$

and

$$E_D^b = \frac{1}{2} \sum_{j=1}^b \sum_{k=1}^{N_b} (\mathcal{B}_j(\mathbf{x}_k; \mathcal{N}(\mathbf{x}_k, \mathbf{w}), \partial\mathcal{N}(\mathbf{x}_k, \mathbf{w}), \partial\partial\mathcal{N}(\mathbf{x}_k, \mathbf{w})))^2, \quad (8)$$

where

$$E = \beta_q E_D^q + \beta_b E_D^b \quad (9)$$

By $N_{q/b}$, we denote a number of points in $\mathcal{M}/\partial\mathcal{M}$ collected to optimize the network model. The total training dataset consists of points from \mathcal{M} and $\partial\mathcal{M}$, namely, $\mathcal{D} = \mathcal{D}_q \cup \mathcal{D}_b$.

3 Bayesian framework for neural networks

Solving the PDE in the PINN approach comes down to optimization tasks. Namely, it is assumed that the neural network parameterizes the solution, then the loss, such as in Eq. 6, is formulated, and model parameters are optimized. Solving the PDE can be understood as the Bayesian inference process. Indeed, we assume prior knowledge about the solution and its parameters and then search for the posterior realization. Another problem is the proper fine-tuning of the beta parameters, which controls the impact of the boundary conditions on the solution. The choice of optimal network architecture seems to be essential too. Eventually, it is evident that the solution given by the neural network is only an approximation of the *true* solution, or it can be treated as a statistical prediction of the desired solution. Therefore, the PINN solution should be provided with uncertainties. We shall argue in the next section that the Bayesian statistical methods can help to establish the optimal structure of the network architecture; moreover, with the help of Bayesian reasoning, one may obtain the optimal values for the hyperparameters such as β_q and β_b , and α (a decay width) and compute uncertainties for the obtained fits.

3.1 General foundations

The Bayesian framework [50, 51, 52, 32] we adapt aims to obtain the posterior densities for the network parameters, weights \mathbf{w} , and hyperparameters $\boldsymbol{\alpha}$ and $\boldsymbol{\beta}$.

A choice of network architecture impacts the analysis results. Indeed, a model that is too simple, with a small number of neurons, cannot be flexible enough to describe the problem. On the other hand, a model that is too complex, with many neurons, may tend to overfit the data and, as a result, not interpolate well between grid points. As we mentioned above, BF shall allow us to compare fits obtained for different networks and get posterior densities for all necessary model parameters and hyperparameters.

In the BF the posteriors for the model parameters and hyperparameters are obtained in the ladder approximation described below. Finally, the approach leads to the computation of the so-called evidence, a measure that ranks models.

The starting point of the procedure is to obtain the posterior density for the network weights. Assuming that the hyperparameters, $\boldsymbol{\alpha}$ and $\boldsymbol{\beta}$, and model architecture \mathcal{N} are fixed

$$P(\mathbf{w} \mid \boldsymbol{\alpha}, \boldsymbol{\beta}, \mathcal{N}, \mathcal{D}) = \frac{P(\mathcal{D} \mid \mathbf{w}, \boldsymbol{\beta}, \mathcal{N})P(\mathbf{w} \mid \boldsymbol{\alpha}, \mathcal{N})}{P(\mathcal{D} \mid \boldsymbol{\alpha}, \boldsymbol{\beta}, \mathcal{N})} \quad (10)$$

$$P(\mathcal{D} \mid \boldsymbol{\alpha}, \boldsymbol{\beta}, \mathcal{N}) = \int P(\mathcal{D} \mid \mathbf{w}, \boldsymbol{\beta}, \mathcal{N})P(\mathbf{w} \mid \boldsymbol{\alpha}, \mathcal{N})d\mathbf{w}. \quad (11)$$

In the above, we silently assumed that the hyperparameter $\boldsymbol{\beta}$ appears in the likelihood $P(\mathcal{D} \mid \mathbf{w}, \boldsymbol{\beta}, \mathcal{N})$, while hyperparameter $\boldsymbol{\alpha}$ appears in prior $P(\mathbf{w} \mid \boldsymbol{\alpha}, \mathcal{N})$ only.

In principle, the hyperparameters should be integrated from the model's prior densities, but usually, it is either difficult or impossible to perform. In the BF framework, it is assumed that the posterior density $p(\boldsymbol{\alpha}, \boldsymbol{\beta} | \mathcal{N}, \mathcal{D})$ has a sharp peak at $\boldsymbol{\alpha}_{MP}, \boldsymbol{\beta}_{MP}$ (MP - maximum of posterior) then prior for weights reads $p(\mathbf{w} | \mathcal{N}, \mathcal{D}) \approx p(\mathbf{w} | \boldsymbol{\alpha}_{MP}, \boldsymbol{\beta}_{MP}, \mathcal{N}, \mathcal{D})$ (in reality, the posterior has many sharps peaks, we comment on that in the following section). Note that the Gaussian approximation makes sense as long as the number of weights is smaller than the number of data constraints [52]. We see that to obtain the desired prior, one needs to find $\boldsymbol{\alpha}_{MP}, \boldsymbol{\beta}_{MP}$.

In the second step, we use the likelihood for the hyperparameters, Eq. 11, to evaluate the posterior density for the hyperparameters, namely,

$$P(\boldsymbol{\alpha}, \boldsymbol{\beta} | \mathcal{N}, \mathcal{D}) = \frac{P(\mathcal{D} | \boldsymbol{\alpha}, \boldsymbol{\beta}, \mathcal{N})P(\boldsymbol{\alpha}, \boldsymbol{\beta} | \mathcal{N})}{P(\mathcal{D} | \mathcal{N})} \quad (12)$$

$$P(\mathcal{D} | \mathcal{N}) = \int P(\mathcal{D} | \boldsymbol{\alpha}, \boldsymbol{\beta}, \mathcal{N})P(\boldsymbol{\alpha}, \boldsymbol{\beta} | \mathcal{N})d\boldsymbol{\alpha} d\boldsymbol{\beta} \quad (13)$$

Note that the density (13) is called the model evidence. In reality, the prior for the hyperparameters factorizes into the product of two densities, namely,

$$P(\boldsymbol{\alpha}, \boldsymbol{\beta} | \mathcal{N}) = P(\boldsymbol{\alpha} | \mathcal{N})P(\boldsymbol{\beta} | \mathcal{N}). \quad (14)$$

In the third step, we compute the posterior density $P(\mathcal{N} | \mathcal{D})$. It is the quantity that ranks the models, i.e., a model the most favorable by the data has the highest value of $P(\mathcal{N} | \mathcal{D})$.

$$P(\mathcal{N} | \mathcal{D}) = \frac{P(\mathcal{D} | \mathcal{N})P(\mathcal{N})}{P(\mathcal{D})}. \quad (15)$$

In practice, any model is equally likely at the beginning of the analysis, and $P(\mathcal{N})$ is uninformative. Hence

$$P(\mathcal{N} | \mathcal{D}) \sim P(\mathcal{D} | \mathcal{N}) \quad (16)$$

and to rank the model, it is enough to compute the evidence.

3.2 Implementation of Bayesian framework

This section summarizes the main steps of the BF. See chapter 10 of [32] for more details. The main idea is to assume that all the densities should have a Gaussian-like shape. The inference process of estimating optimal weights, hyperparameters, and model structure can be split into three steps announced in the previous section.

First step

The prior density for the weights is constructed based on several observations. Namely, a network works the most efficiently for weights parameters that take values around zero. There are no sign preferences for the weights. Moreover, one can distinguish several classes of weights in the network. It is the result of the internal symmetries of a network model. For instance, the interchange of two units in the same hidden layer does not change the functional form of the network map. The weights which belong to the same class should have the same scaling property [32]. According to that, we assume the following Gaussian prior density for the weights:

$$p(\mathbf{w} | \boldsymbol{\alpha}, \mathcal{N}) = \frac{1}{Z_W} \exp\left(-\sum_{i=1}^C \alpha_i E_w^i\right) \equiv \frac{1}{Z_W} \exp(-E_w), \quad (17)$$

and

$$E_w^i = \frac{1}{2} \sum_{k=s_{i-1}}^{s_i} w_k^2, \quad s_i = \sum_{l=1}^i W_l, \quad s_0 = 1 \quad (18)$$

$$Z_W(\boldsymbol{\alpha}) = \prod_{i=1}^C \left(\frac{2\pi}{\alpha_i}\right)^{\frac{w_i}{2}}, \quad (19)$$

In the above, C denotes the number of weight classes; w_j refers to the j -th weight, W_i is the number of weights in i -th class; α_i is a decay width for i -th class of weights. The vector $\boldsymbol{\alpha} = (\alpha_1, \dots, \alpha_C)$ contains decay weights.

Note that the α_i 's play two roles. They control the underfitting/overfitting. If α is too small, the network tends to overfit, whereas when α is too large, the network does not adapt to the data. The $1/\sqrt{\alpha_i}$'s defines the width of the Gaussian prior for weights.

Now, we shall construct the likelihood so that it contains all the contributions of the PINN loss terms. Assume that we have the constraints coming from the differential equations and one determined by the boundary condition, then we have two corresponding hyper-parameters β_q, β_b , and the likelihood reads

$$p(\mathcal{D} | \mathbf{w}, \boldsymbol{\beta}) = \frac{1}{Z_D(\boldsymbol{\beta})} \exp(-\beta_q E_D^q - \beta_b E_D^b), \quad (20)$$

where the normalization factor reads

$$Z_D(\boldsymbol{\beta}) = Z_D(\beta_q) Z_D(\beta_b) \quad (21)$$

and

$$Z_D(\beta_{q(b)}) = \left(\frac{2\pi}{\beta_{q(b)}} \right)^{\frac{N_{q(b)}}{2}}. \quad (22)$$

Having the posterior and the likelihood, we compute the posterior for the weights

$$p(\mathbf{w} | \mathcal{D}, \boldsymbol{\alpha}, \boldsymbol{\beta}) = \frac{p(\mathcal{D} | \mathbf{w}, \boldsymbol{\beta}) p(\mathbf{w}, \boldsymbol{\alpha})}{\int d\mathbf{w} p(\mathcal{D} | \mathbf{w}, \boldsymbol{\beta}) p(\mathbf{w}, \boldsymbol{\alpha})} \quad (23)$$

$$= \frac{1}{Z_T(\boldsymbol{\alpha}, \boldsymbol{\beta})} \exp\left(-\left\{\sum_{i=1}^C \alpha_i E_w^i + \beta_q E_D^q + \beta_b E_D^b\right\}\right), \quad (24)$$

where

$$E_T = \sum_{i=1}^C \alpha_i E_w^i + \beta_q E_D^q + \beta_b E_D^b \quad (25)$$

$$Z_T(\boldsymbol{\alpha}, \boldsymbol{\beta}) = \int d\mathbf{w} \exp(-E_T(\mathbf{w})). \quad (26)$$

Then it is assumed that the posterior has a sharp local maximum and to estimate it, one expands the E_T around its minimum

$$E_T(\mathbf{w}) \approx E_T(\mathbf{w}_{MP}) + \frac{1}{2} (\mathbf{w} - \mathbf{w}_{MP})^T \mathbf{A} (\mathbf{w} - \mathbf{w}_{MP}), \quad (27)$$

where \mathbf{A} is defined by

$$\mathbf{A} = \mathbf{H} + \mathbf{I}_W(\boldsymbol{\alpha}), \quad (28)$$

where

$$\mathbf{I}_W(\boldsymbol{\alpha}) = \text{diag}(\underbrace{\alpha_1, \dots, \alpha_1}_{W_1 \text{ times}}, \dots, \underbrace{\alpha_C, \dots, \alpha_C}_{W_C \text{ times}}) \quad (29)$$

and

$$\mathbf{H}_{ij} = \beta_q \nabla_i \nabla_j E_D^q + \beta_b \nabla_i \nabla_j E_D^b \quad (30)$$

is the Hessian.

Within the above approximation, one gets:

$$p(\mathbf{w} | \mathcal{D}, \boldsymbol{\alpha}, \boldsymbol{\beta}) = \frac{1}{Z_{E_T}^*} \exp\left(-E_T(\mathbf{w}_{MP}) - \frac{1}{2} (\mathbf{w} - \mathbf{w}_{MP})^T \mathbf{A} (\mathbf{w} - \mathbf{w}_{MP})\right), \quad (31)$$

where $Z_{E_T} \rightarrow Z_{E_T}^*$,

$$Z_{E_T}^* = \exp(-E_T(\mathbf{w}_{MP})) \sqrt{\frac{(2\pi)^W}{|\mathbf{A}|}}. \quad (32)$$

$|\mathbf{A}|$ is determinant of matrix \mathbf{A} . Eventually, we obtain the posterior

$$p(\mathbf{w} | \mathcal{D}, \boldsymbol{\alpha}, \boldsymbol{\beta}) = \sqrt{\frac{|\mathbf{A}|}{(2\pi)^W}} \exp\left(-\frac{1}{2}(\mathbf{w} - \mathbf{w}_{MP})^T \mathbf{A}(\mathbf{w} - \mathbf{w}_{MP})\right). \quad (33)$$

Note that to find the \mathbf{w}_{MP} , we shall find the minimum of the loss (25).

Before we review the next steps of the approximation, let us comment on the validity of the Gaussian approximation. In neural network analyses, the error function has many minima, some related to symmetry property embodied by a particular type of network architecture. There are local minima that are not related by symmetry. As proposed in [52, 69, 32], one may consider every local minimum (maximum of the posterior), not related by symmetry, as a separate model configuration with its own optimal hyperparameter configuration. It may happen that distinct \mathbf{w}_{MP} (not related by symmetry property) can have different hyperparameters $\boldsymbol{\alpha}_{MP}$, $\boldsymbol{\beta}_{MP}$. From that perspective, the integrals such as Eq. 13 should be interpreted as integral over the neighborhood of the optimal parameters of the local minimum. In such approximation, one collects parameter and hyperparameter configurations corresponding to some local maxima of posterior densities.

Second step

Given optimal configuration of \mathbf{w}_{MP} should have corresponding optimal hyperparameters $\boldsymbol{\alpha}_{MP}$, $\boldsymbol{\beta}_{MP}$ which sit in local maximum of the posterior $p(\boldsymbol{\alpha}, \boldsymbol{\beta} | \mathcal{N}, \mathcal{D})$. We have limited prior knowledge about the hyperparameters, so non-informative priors are discussed [70]. Usually, all (positive) values of hyperparameters are assumed to be allowed. As a result, the likelihood density $p(\mathcal{D} | \boldsymbol{\alpha}, \boldsymbol{\beta}, \mathcal{N})$, for given optimal value of weights, should have the peak in the same position as posterior $p(\boldsymbol{\alpha}, \boldsymbol{\beta} | \mathcal{N}, \mathcal{D})$.

Below we shall obtain hyperparameters into so-called evidence approximation [36, 51]. Taking into account all the above as well as the results of the previous step one estimates the integral

$$p(\mathcal{D} | \boldsymbol{\alpha}, \boldsymbol{\beta}, \mathcal{N}) = \int d\mathbf{w} p(\mathcal{D} | \mathbf{w}, \boldsymbol{\beta}) p(\mathbf{w} | \boldsymbol{\alpha}, \mathcal{N}) = \frac{Z_{E_T}^*}{Z_D(\boldsymbol{\beta}) Z_W(\boldsymbol{\alpha})}, \quad (34)$$

where it was assumed that prior depends only on $\boldsymbol{\alpha}$ whereas the likelihood on $\boldsymbol{\beta}$ only. Then one gets

$$\ln p(\mathcal{D} | \boldsymbol{\alpha}, \boldsymbol{\beta}, \mathcal{N}) \approx -\sum_{i=1}^C \alpha_i E_w^i(\mathbf{w}_{MP}) - \beta_q E_D^q(\mathbf{w}_{MP}) - \beta_b E_D^b(\mathbf{w}_{MP}) \quad (35)$$

$$-\frac{1}{2} \ln |\mathbf{A}| - \sum_{i=1}^C \frac{W_i}{2} \ln \left(\frac{2\pi}{\alpha_i} \right) - \frac{N_q}{2} \ln \left(\frac{2\pi}{\beta_q} \right) - \frac{N_b}{2} \ln \left(\frac{2\pi}{\beta_b} \right).$$

We search for the maximum of $p(\mathcal{D} | \boldsymbol{\alpha}, \boldsymbol{\beta}, \mathcal{N})$, in the original MacKay's framework, the hyperparameters are iterated according to the necessary condition for the maximum, namely from the equations:

$$\frac{\partial}{\partial \boldsymbol{\alpha}} p(\mathcal{D} | \boldsymbol{\alpha}, \boldsymbol{\beta}, \mathcal{N}) = 0, \quad \frac{\partial}{\partial \boldsymbol{\beta}} p(\mathcal{D} | \boldsymbol{\alpha}, \boldsymbol{\beta}, \mathcal{N}) = 0.$$

In our approach, we propose to consider additional loss given by $E_{hyp} = -\ln p(\mathcal{D} | \boldsymbol{\alpha}, \boldsymbol{\beta})$ and optimize it with respect to hyperparameters. The loss, after neglecting constant terms, has the form

$$\begin{aligned} E_{hyp} &= \sum_{i=1}^C \alpha_i E_w^i(\mathbf{w}_{MP}) + \beta_q E_D^q(\mathbf{w}_{MP}) + \beta_b E_D^b(\mathbf{w}_{MP}) + \frac{1}{2} \ln |\mathbf{A}| \\ &\quad - \sum_{i=1}^C \frac{W_i}{2} \ln \alpha_i - \frac{N_q}{2} \ln \beta_q - \frac{N_b}{2} \ln \beta_b. \end{aligned} \quad (36)$$

Note that the above algorithm obtains the hyperparameters alphas and betas. The first type of parameter controls the impact of the prior on the posterior, and the optimal solution should be the one for which the model generalizes well. The beta parameters give information about the noise in the data; however, this information is partial as long as the number of data points is not large. On the other hand, the algorithm gets the beta parameters so that they maximize the evidence for a given model. Hence, the algorithm finds a balance between various posterior contributions in order to get the model with the best generalization abilities (in this case, mostly interpolation).

Third step

To compute the evidence, one has to integrate out the hyperparameters from $p(\mathcal{D} \mid \boldsymbol{\alpha}, \boldsymbol{\beta}, \mathcal{N})$ using the similar arguments as for the prior for the weights, namely, the posterior for the hyperparameters has a sharp peak in their parameters. As it is argued in [32, 70] are the scaling parameters that are always positive. Therefore, instead of considering $p(\mathcal{D} \mid \boldsymbol{\alpha}, \boldsymbol{\beta}, \mathcal{N}) d\boldsymbol{\alpha} d\boldsymbol{\beta}$, one discusses $p(\mathcal{D} \mid \ln \boldsymbol{\alpha}, d \ln \boldsymbol{\beta}, \mathcal{N}) d \ln \boldsymbol{\alpha} d \ln \boldsymbol{\beta}$. Then it is assumed that the prior for \ln of hyperparameters is flat. As a result, the log of evidence reads

$$\ln p(\mathcal{D} \mid \mathcal{N}) = \ln p(\mathcal{D} \mid \boldsymbol{\alpha}, \boldsymbol{\beta}) + \ln \sigma_{\ln \alpha} + \ln \sigma_{\ln \beta_{E_q}} + \ln \sigma_{\ln \beta_b} + \text{comb}, \quad (37)$$

where

$$\begin{aligned} \ln p(\mathcal{D} \mid \boldsymbol{\alpha}, \boldsymbol{\beta}) &= - \sum_{i=1}^C \alpha_i E_w^i(\mathbf{w}_{MP}) - \beta_{E_q} E_D^q(\mathbf{w}_{MP}) - \beta_b E_D^b(\mathbf{w}_{MP}) \\ &\quad - \frac{1}{2} \ln |\mathbf{A}| + \sum_{i=1}^C \frac{W_i}{2} \ln \alpha_i + \frac{N_q}{2} \ln \beta_q + \frac{N_b}{2} \ln \beta_b \end{aligned} \quad (38)$$

and

$$\ln \sigma_{\ln \alpha_i} = -\frac{1}{2} \ln \left[-\alpha_i^2 \frac{\partial^2}{\partial \alpha_i^2} \ln p(\mathcal{D} \mid \boldsymbol{\alpha}, \boldsymbol{\beta}) \right], \quad (39)$$

$$\ln \sigma_{\ln \beta_i} = -\frac{1}{2} \ln \left[-\beta_i^2 \frac{\partial^2}{\partial \beta_i^2} \ln p(\mathcal{D} \mid \boldsymbol{\alpha}, \boldsymbol{\beta}) \right]. \quad (40)$$

The expression (37) consists of the symmetry contribution, as discussed in Ref. [71], namely,

$$\text{comb} = \sum_{i=1}^L (\ln M_i! + M_i \ln 2), \quad (41)$$

where M_i denotes number of units in the i -th hidden layer, L denotes number of hidden layers.

Uncertainty for the network predictions

The Bayesian approach to neural networks can take into account two types of uncertainties, namely, aleatoric and epistemic [35]. The first has roots in the data, the other in the model and its parameters dependence. In our case, we rather concentrate on the epistemic uncertainties. The Bayesian framework we adapted can estimate the uncertainty due to model dependence (given by evidence) and parameter dependence. The latter can be computed in the covariance matrix approximation. Indeed, the 1σ uncertainty due to the variation of the weights reads [72]

$$\Delta^2 \mathcal{N}(\mathbf{x}_{q(b)}, \mathbf{w}_{MP}) = \sum_{i,j} \nabla_i \mathcal{N}(\mathbf{x}_{q(b)}, \mathbf{w}_{MP}) (\mathbf{A}^{-1})_{ij} \nabla_j \mathcal{N}(\mathbf{x}_{q(b)}, \mathbf{w}_{MP}), \quad (42)$$

where $\mathbf{x}_{q(b)}$ refers to point from $\mathcal{M}(\partial \mathcal{M})$; $\nabla_i \equiv \partial / \partial w_i$.

3.3 Training algorithm

Here, we briefly summarize the training algorithm.

- Set the network architecture and initial values for the weights.
- Set initial values of $\alpha_i = \alpha_i^{(0)}$ and $\beta_a = \beta_a^{(0)}$.
- To get \mathbf{w}^* minimize the loss (25).
- To get hyperparameters α and β minimize the loss (36).
- The best network has the highest evidence value computed from (37).

* In both optimizations Adam algorithm [73] was utilized.

Note that during the training process, one has to update weights and the values of hyperparameters simultaneously. However, searching for optimal hyperparameters' optimal configuration for given \mathbf{w}_{MP} makes numerical sense when one is close to the peak of the posterior. The Adam algorithm we use is rather slow in approaching the minimum. Therefore, we start the optimization of weights after some number of epochs of optimization. Eventually, we optimize the hyperparameters every several epochs; otherwise, the procedure can be unstable. In our previous analyses, we considered the Lavenberg-Marquadt algorithm [57], which is fast approaching the minimum of the loss function. In that case, we updated hyperparameters for every epoch. Note that the simultaneous weight update and hyperparameters update can be understood as a bi-level optimization problem [74].

4 Numerical experiments

We will solve three types of partial differential equations: heat, wave, and Burger's. Analytic solutions are available for the first two equations, but there is no analytical solution for Burger's equation. To approach this problem, we have used the PyTorch framework [59], and collected 100 solutions for each of the three PDEs. We will be selecting the best solution based on the evidence.

Before discussing the results for PDEs, we will begin the presentation by comparing our framework to the Bayesian approach based on the Markov chain algorithm. We will apply both methods to fit a curve. Next, we will simplify our approach to solving the heat equation by considering only one hyperparameter α and one β . We will repeat this scenario for the wave equation as well. Then, we solve the wave equation within the full model, keeping all allowed weight decay parameters and beta's. Finally, we shall solve Burger's equation with the semi-simplified version of our approach, where we consider one weight decay hyperparameter α and several beta parameters that control the equation and boundary condition and additional data contributions. Indeed, in the last example, we study the problem, in which we also have additional information coming from the "measured" data. Namely, we add the information about the solution with some uncertainty to the analysis. This additional contribution is provided with a corresponding β hyperparameter, which is tuned within the Bayesian algorithm.

4.1 Comparison with HMC

Let us compare the results of the Bayesian approach introduced in the previous section with the Bayesian approach in which the posterior distributions are sampled using the Hybrid Monte Carlo (HMC) algorithm [44, 75]. This approach is adapted in Ref. [45] to formulate the B-PINN framework. In the HMC approach, there is no need to make simplifications in evaluating the posteriors. However, as in the Bayesian framework presented in this paper, fixing the hyperparameters like α and β requires additional care [44].

To compare the predictions of both approaches, we consider the nonlinear regression problem. Let us consider the curve parametrized as follows

$$u(x) = x^2 \cos^2(4x). \quad (43)$$

To generate the data we compute $u_{data}(x_i) = u(x_i) + \epsilon_i$, where ϵ_i is drawn from the normal distribution with zero mean and 0.05 variance, whereas x_i are obtained in the following way: 12 points are drawn from the interval $[-0.8, -0.3]$ and 12 points are drawn from the interval $[0.3, 0.8]$.

We fit the data with a one-hidden-layer neural network consisting of six hidden units. The hyperbolic tangent gives the activation functions. We trained some number of networks, each of them for 15000 epochs. We show the best fit according to evidence. We switched on the Bayesian algorithm to evaluate hyperparameters after the 1000th epoch and converged at $\alpha = 0.24$, $\beta = 596$.

For the HMC approach, we take the same network architecture and hyperparameters α and β as in the previous analysis. To obtain the HMC fit, we draw from the posterior 15000 samples. The mean over collected samples (with 1000 burn steps) gives the model response as a final result. The corresponding variance determines the uncertainty.

Both fits are depicted in Fig. 2. As we see, both approaches lead to similar fits and comparable uncertainties. However, one can expect that for more complex problems, the uncertainties computed

from the HMC approach would be more prominent than in this paper’s approach. Indeed, in our approach, we focus on the local posterior peak, and assume that it has a Gaussian-like shape.

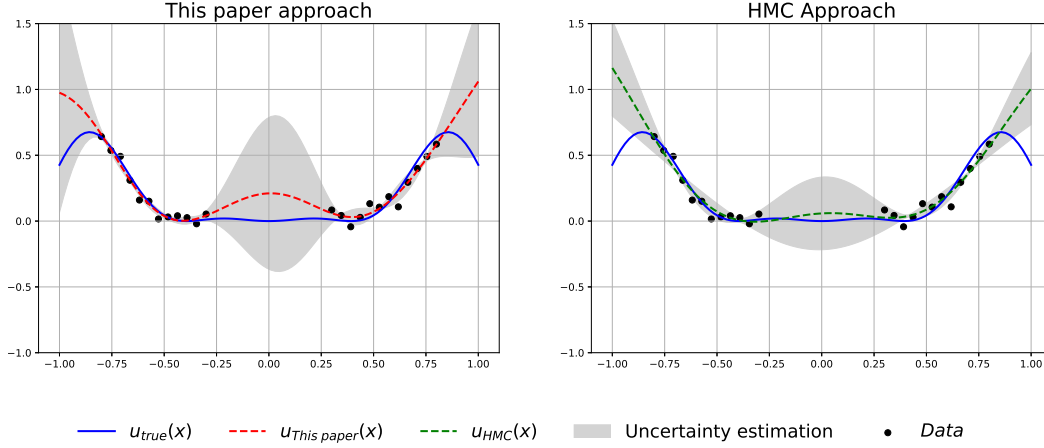


Figure 2: Nonlinear regression within this paper approach (left panel) and HMC approach (right panel). The red/blue line corresponds to this paper/HMC fit. The solid blue line describes the true value.

On the other hand, in the HMC approach, there is no clear guideline for tuning hyperparameters. Additionally, the HMC algorithm’s parameters, namely, number of samples, and the hyperparameters, such as the number of leapfrog steps, require estimation.

4.2 Heat equation

Let us consider the heat equation of the form

$$\frac{\partial u}{\partial t} - \kappa \frac{\partial^2 u}{\partial x^2} = 0, \quad x \in [0, 1], \quad t \in [0, 1], \quad (44)$$

$$u(0, t) = u(1, t) = 0, \quad (45)$$

$$u(x, 0) = \sin(\pi x) \quad (46)$$

For the above case the analytic solution reads $u_{true}(x, t) = \sin(\pi x) \exp(-\kappa\pi^2 t)$.

We consider a small network with one hidden layer to solve the heat equation (44) with boundary conditions (45-46). The hidden layer has six neurons with hyperbolic tangent activation functions. In the output layer, there is no activation function.

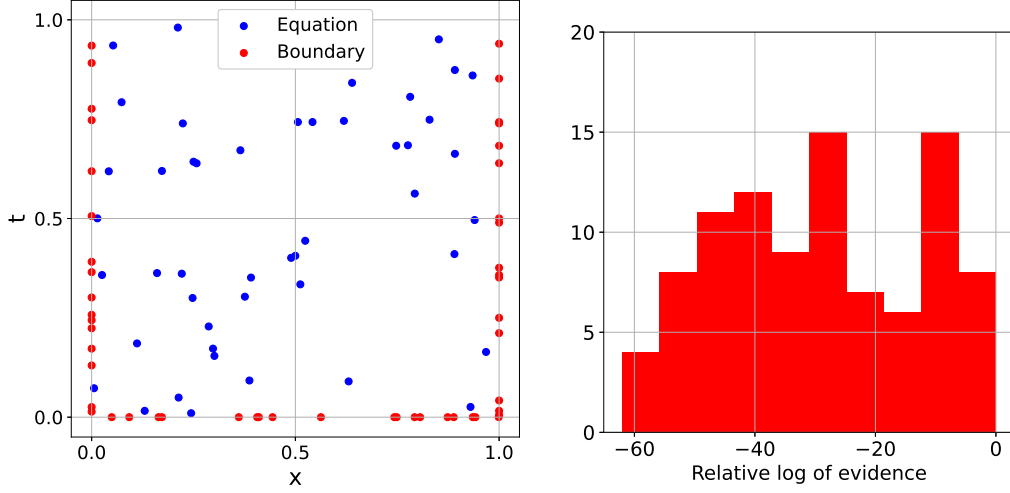


Figure 3: In the left panel: the training data, the blue/red points correspond to the equation/boundary contribution to the loss for the heat equation. In the right panel: the histogram of the relative log of evidence (the difference between a given log of evidence and the highest log of evidence).

The data on the boundary Eqs. (45-46) were randomly drawn from the uniform distribution (50 points). Similarly, we obtained data in $(0, 1) \times (0, 1)$ (50 points). The data considered in the training are shown in Fig. 3 (left panel).

Here, the Bayesian training was performed in the simplest fashion. Namely, we kept one α parameter for all weight classes (as in Ref. [3]) and one $\beta = \beta_q = \beta_b$ for equation and boundary contribution.

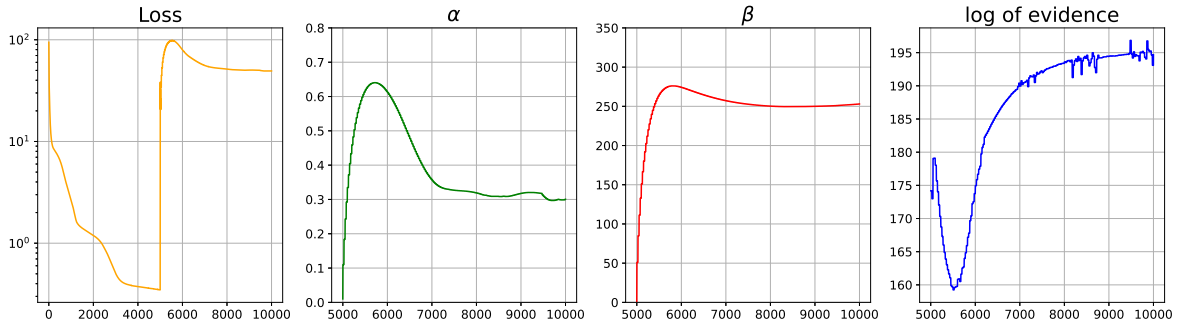


Figure 4: An example of loss E_T (the first panel in the left), E_{hyp} (the last panel) and α (the second from the right) and β (the third from the right) hyperparameters evolution during the training of the network that solves the heat equation.

We optimized the hyperparameters after 5000 epochs to maintain the procedure's convergence. Then, every 25 epoch, we updated the α and β parameters to minimize the error E_{hyp} . In Fig. 4, we show, one of the registered training examples. The method leads to the convergence of both discussed losses E_T and E_{hyp} with respect to weights and hyperparameters, respectively. We started the optimization from a low value of α (minor relevance of the penalty term). During the training, α changes by the order of magnitude. The β parameter slowly varies during the optimization process.

For every fit, we compute the evidence. In Fig. 3 (right panel), we show the histogram of evidence values for 100 models. The best model has the highest evidence. In Fig. 5 we show our best fit together with the exact analytic solution. The fit is plotted together with 2σ uncertainty. Note that we show the x -dependence of the solution in five time steps.

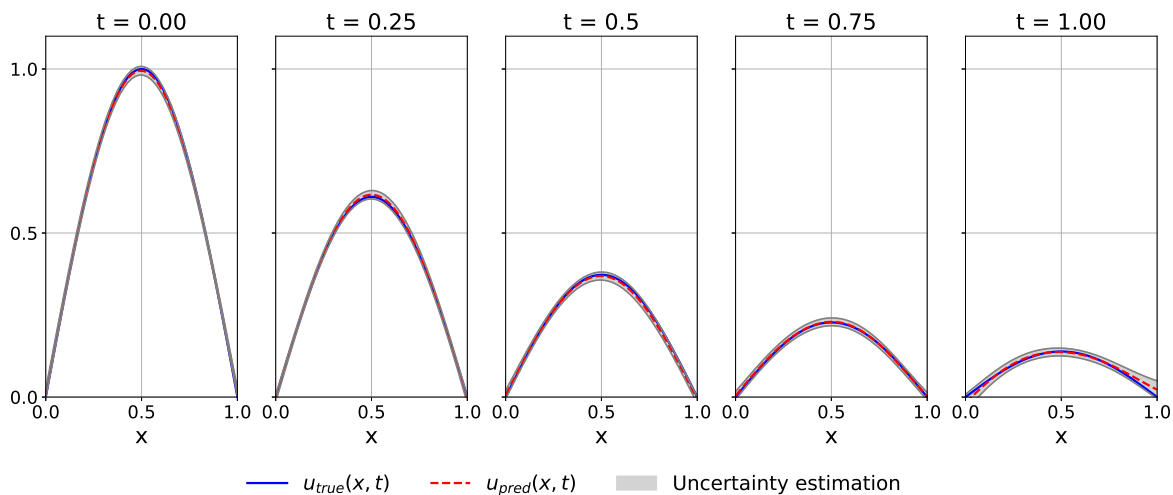


Figure 5: The exact (u_{true}) and PINN (u_{pred}) solutions for the heat equation. The grey area denotes 2σ uncertainty.

4.3 Wave equation

Let us consider the following wave equation

$$\frac{\partial^2 u}{\partial t^2} - \frac{\partial^2 u}{\partial x^2} = 0, \quad x \in [0, 1], \quad t \in [0, 1] \quad (47)$$

$$u(0, t) = u(1, t) = 0 \quad (48)$$

$$\frac{\partial}{\partial t} u(0, t) = 0 \quad (49)$$

with

$$u(x, 0) = \sin(\pi x) + \frac{1}{2} \sin(2\pi x). \quad (50)$$

The analytic solution reads $u_{true}(x, t) = \sin(\pi x) \cos(\pi t) + \frac{1}{2} \sin(2\pi x) \cos(2\pi t)$.

In the previous subsection, we demonstrated that the BF is effective for solving the heat equation. The solution could be obtained by using a relatively small network, and the optimization process took rather small number of epochs. However, solving the wave equation using BF was found to be more challenging. We used a network with one hidden layer containing eighth hidden units, and the hyperbolic tangent was used as the activation function in the hidden layer. To get a successful fit, we generated a dataset of the same size as the heat equation problem. The dataset consisted of 50 points for \mathcal{M} and 50 points for $\partial\mathcal{M}$, drawn from a uniform distribution. We also considered more points for the initial condition at $t = 0$. The dataset's distribution is shown in the left panel of Fig. 6.

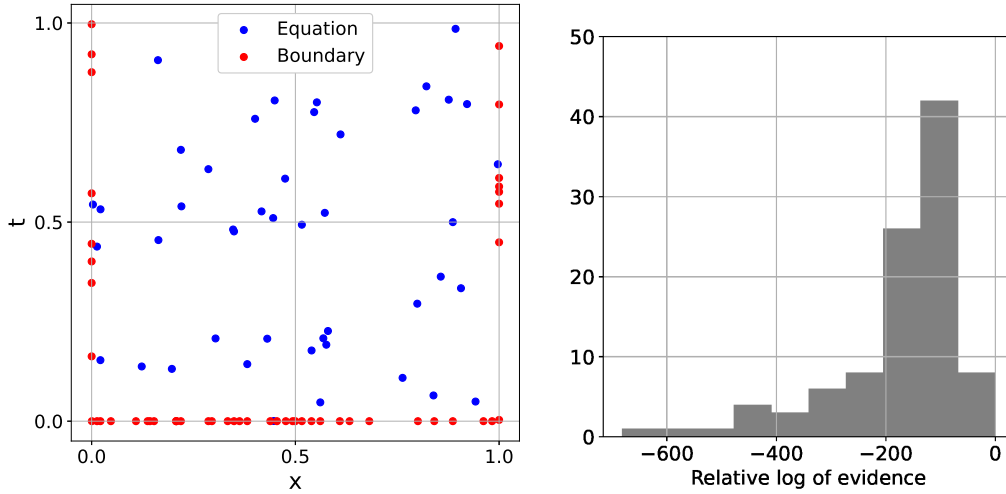


Figure 6: In the left panel: the training data, the blue/red points correspond to equation/boundary contribution to the loss for the wave equation. In the right panel: the histogram of the relative log of evidence (the difference between a given log of evidence and the highest log of evidence).

The wave equation with boundary condition (50) was solved in the simplified framework with only one α and β hyperparameters. For this case, the learning process lasted significantly longer than in the heat equation problem and it took 20000 epochs. We started optimization of the hyperparameters in the 5000th epoch. The best (due to evidence) training example for this case is given in Fig. 7.

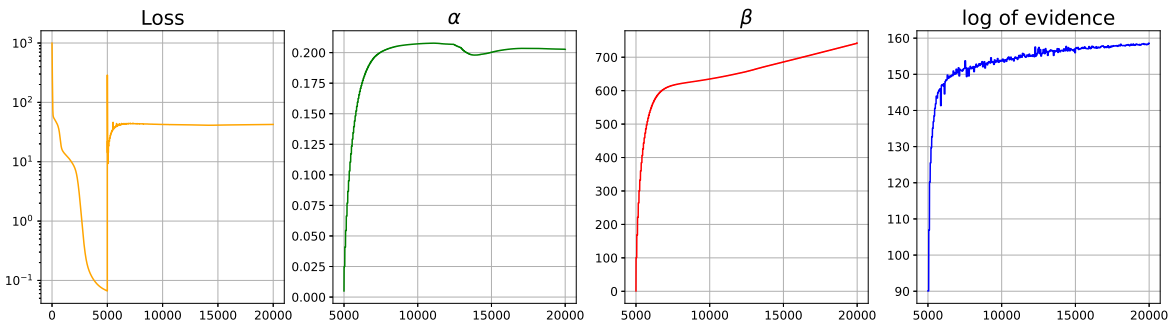


Figure 7: Parameters evolution during the wave equation training for the model with the highest evidence.

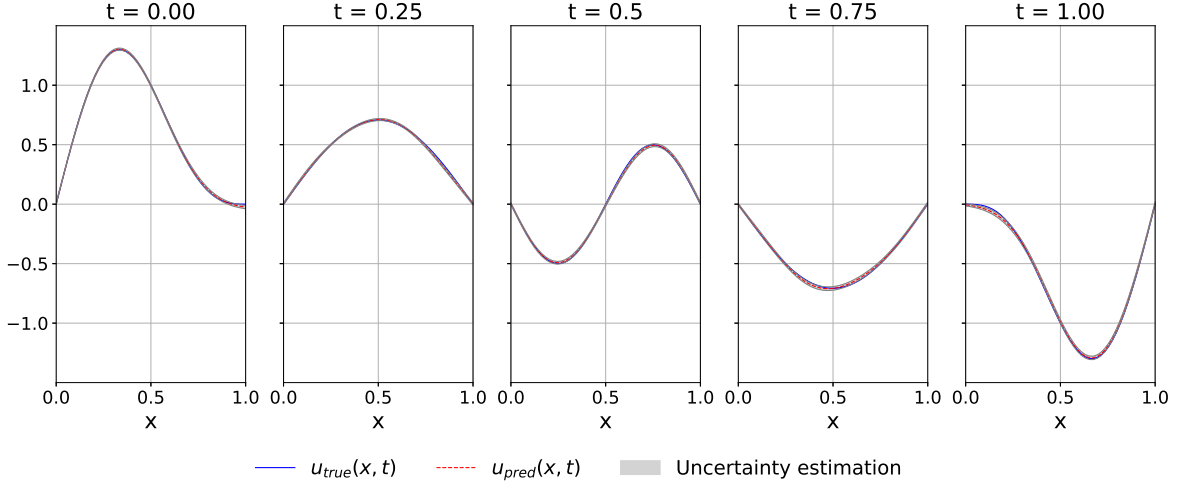


Figure 8: The exact (u_{true}) and PINN (u_{pred}) solutions for the heat equation with boundary conditions (50). The grey area denotes 2σ uncertainty.

Similarly, as for the heat equation, we show the histogram of the relative log of evidence values in the right panel of Fig. 6. Our best fit agrees with the true solution; see Fig. 8. However, one can notice a slight difference between the wave equation’s exact and network model solutions. To visualize this feature, we plot $u_{true}(x, t) - u_{pred}(x, t)$ together with uncertainty in Fig. 9.

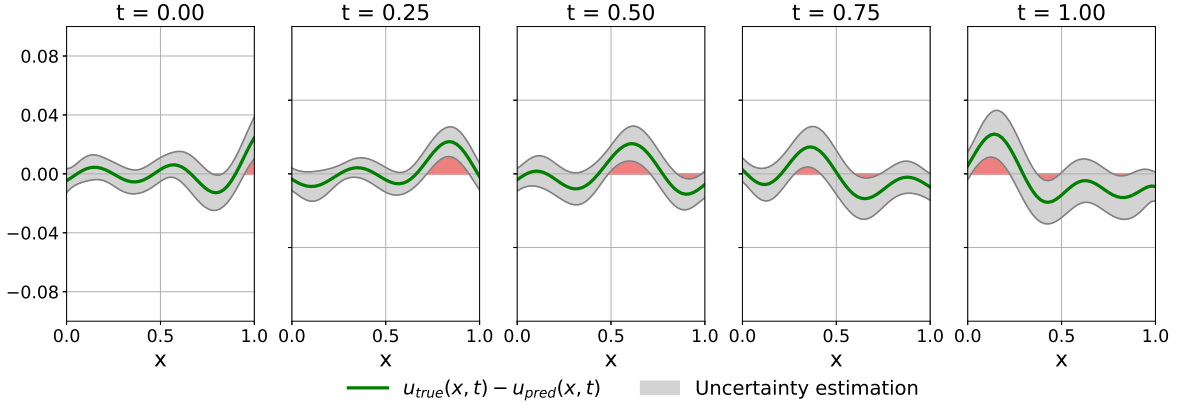


Figure 9: Comparison of the obtained uncertainties and real error for the solution of the wave equation with boundary condition (50). The $y = 0$ axes correspond to the exact agreement between true. The red color indicates where true values are outside the 2σ uncertainty interval.

Keeping more than one α and β parameters complicates the numerical computation, making it more challenging to obtain convergence. However, we performed a complete analysis of the same equation, the dataset, and the training parameters, keeping for every layer of units weights one α and separate α for bias units. We also hold two betas, namely β_q for the equation and β_b for boundary contribution. Hence, we had in the analysis four α parameters (two for the input layer and two for the hidden layer: one for ordinary weights and one for bias weights) and two betas. Again, we considered 100 models in the analysis, and the best-fit evidence (log of) was equal to about 169. In training with one α and one β , the best model had evidence (log of) equal to about 158, which shows that the model with fully allowed hyperparameters is more favorable by the Bayesian algorithm. The parameters evolution during the training is shown in Fig. 10. Optimizing the model leads to the convergence of the loss and log of evidence. When one approaches the minimum of the loss, the boundary constraints’ importance becomes increasingly important; in fact, β_b is almost twice as large as β_q , when the number of data points from both contributions is the same.

To summarize this section, the approach used here is quite effective. However, in the more complex numerical applications, we'll simplify things by only considering a single regularizer, denoted by α , and a complete set of beta parameters. In this scenario, we can effectively regulate the model with all the hyperparameters that describe the equation and boundary constraints being tuned by the Bayesian algorithm.

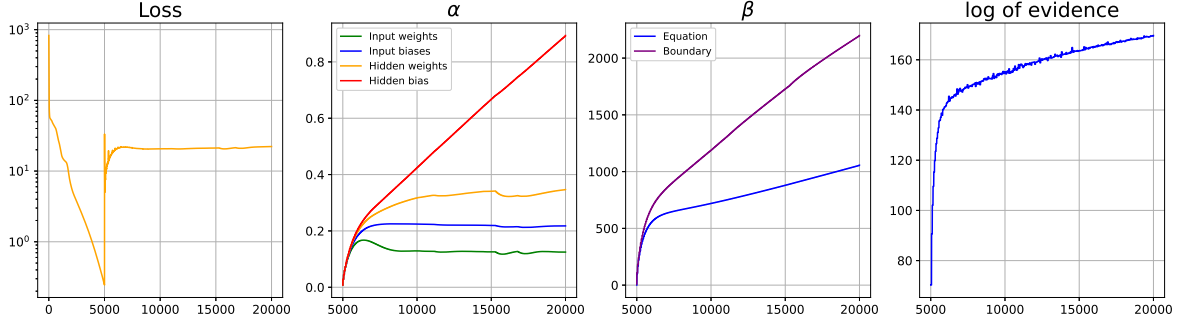


Figure 10: The parameters evolution for the full model. The loss function and evidence reached their plateaus. Although, as one can see the convergence of all parameters was not obtained in the training process.

4.4 Burger's equation

For the last example of PDEs, we consider Burger's equation with Dirichlet boundary conditions.

$$\frac{\partial u}{\partial t} + u \frac{\partial u}{\partial x} - \frac{1}{100\pi} \frac{\partial^2 u}{\partial x^2} = 0, \quad x \in [-1, 1], \quad t \in [0, 1] \quad (51)$$

$$u(0, x) = -\sin(\pi x) \quad (52)$$

$$u(t, -1) = u(t, 1) = 0. \quad (53)$$

It is the same equation as discussed in Ref. [11].

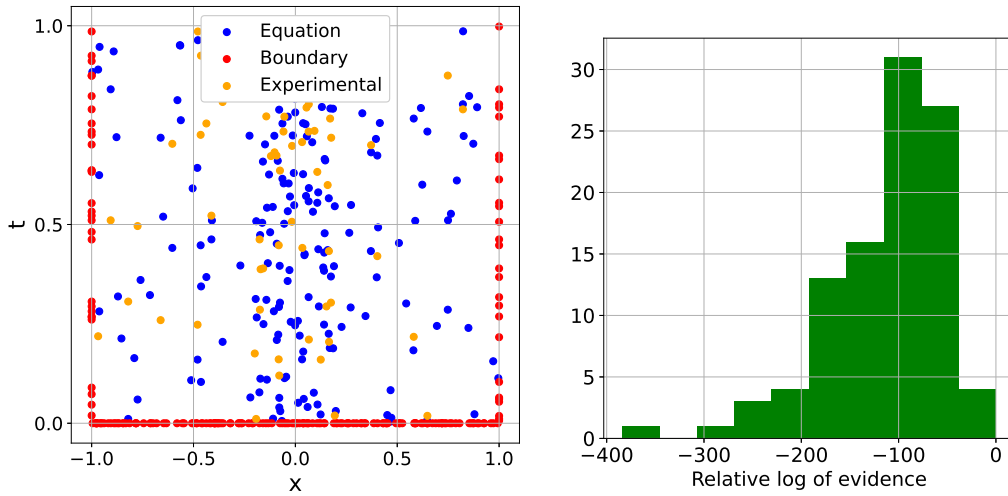


Figure 11: In the left panel: the training data, the blue/red points correspond to the equation/boundary contribution to the loss for Burger's equation. In the right panel: the histogram of the relative log of evidence (the difference between a given and highest log of evidence).

Burger's equation is the most difficult to solve among the three PDEs discussed in this paper. Since the solution's time evolution goes from smooth sine to a very sharp function, solving the problem with

one hidden layer is difficult, so we employed a neural network architecture with two hidden layers with eight units each and, again, hyperbolic tangent as the activation function.

For this problem we consider more general approach, where we have some additional data points. In this case the loss function will be following

$$E_T = \sum_{i=1}^C \alpha_i E_w^i + \beta_q E_D^q + \beta_b E_D^b + \beta_{ex} E_D^{ex}. \quad (54)$$

The dataset contained 200, 200, and 60 points for equation, boundary, and experimental data, respectively. The noise in the “experimental“ data was equal to 0.02. We sampled half of the “experimental“ and equation points from the unitary distribution in the interval $x \in [-0.2, 0.2]$ and the rest from $x \in [-1, 1]$ (t variable is drawn from uniform distribution in $[0, 1]$). Obtaining an accurate solution with limited data was possible when there are enough points near $x = 0$. We show the data distribution in Fig. 11 (left panel).

The networks were trained for 20000 epochs, and we started fitting parameters since the 10000th epoch. In this case we used one α for all weights, but we optimized β_q , β_b , β_{ex} separately.

Similarly, we collected 100 fits for two previous PDEs examples. The histogram of the log of evidence for collected fits is given in Fig. 11 (right panel). In Fig. 12, we show our best fit with the numerical solution obtained in Ref. [11]. A good agreement between the predictions of both approaches is seen.

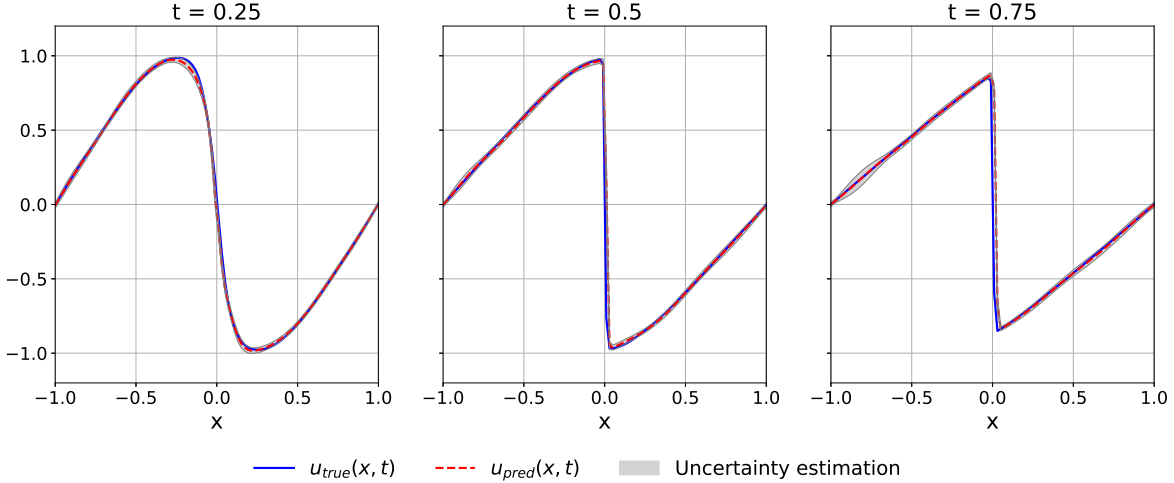


Figure 12: The “true” solution (u_{true}) - the numerical solution from [11], and our best model predictions (u_{pred}) for Burger’s equation. The grey area denotes 2σ uncertainty.

5 Summary

We adopted and modified the Bayesian framework for the PINN to solve heat, wave, and Burger’s equations. The network solutions agree with the “true” ones. The method allowed us to compute the uncertainty due to variation of network parameters, and one may also estimate the variation due to the change in the network architecture. The latter information is encoded in the evidence distribution. Hence, the presented method allows us to estimate epistemic uncertainties.

We have shown that our approach can lead to tuning relative weights between various contributions in the loss function. Our method differs from those of Refs. [61, 62, 63] and [64]. In the last paper, an error function is subject to maximization concerning those parameters. Moreover, the hyperparameters are separately tuned for each data point. To optimize β s, we minimize E_{hyp} , which depends partially linearly on them. But, there is a nonlinear dependence, too, which is hidden in the $\ln |\mathbf{A}|$ and logarithmic contributions. The last two types contribute to the so-called Occam factor and penalize a model formulation that is too complex. Hence, the Bayesian algorithm “chooses” the optimal configuration of conditions according to the delivered information. Note that, in principle, in

the presented Bayesian approach, one would introduce a corresponding hyperparameter for each data point, but studying this problem goes beyond the scope of this paper.

In the present manuscript, we consider shallow neural networks of small sizes. For such architectures, the numerical procedure is effective. Computing the Hessian is accurate and does not take much time. Moreover, as mentioned, the Gaussian approximation makes sense when the number of model parameters is smaller than the number of constraints.

Acknowledgments

K.M.G was supported by the program "Excellence initiative—research university" (2020-2026 University of Wrocław).

References

- [1] Y. LeCun, Y. Bengio, G. Hinton, [Deep learning](#), Nature 521 (2015) 436 EP –.
URL <https://doi.org/10.1038/nature14539>
- [2] P. Mehta, M. Bukov, C.-H. Wang, A. G. Day, C. Richardson, C. K. Fisher, D. J. Schwab, [A high-bias, low-variance introduction to machine learning for physicists](#), Physics Reports 810 (2019) 1 – 124, a high-bias, low-variance introduction to Machine Learning for physicists.
[doi:https://doi.org/10.1016/j.physrep.2019.03.001](https://doi.org/10.1016/j.physrep.2019.03.001).
URL <http://www.sciencedirect.com/science/article/pii/S0370157319300766>
- [3] K. M. Graczyk, P. Plonski, R. Sulej, Neural Network Parameterizations of Electromagnetic Nucleon Form Factors, JHEP 09 (2010) 053. [arXiv:1006.0342](#), [doi:10.1007/JHEP09\(2010\)053](https://doi.org/10.1007/JHEP09(2010)053).
- [4] K. M. Graczyk, C. Juszczak, Proton radius from Bayesian inference, Phys. Rev. C90 (2014) 054334. [arXiv:1408.0150](#), [doi:10.1103/PhysRevC.90.054334](https://doi.org/10.1103/PhysRevC.90.054334).
- [5] K. M. Graczyk, M. Matyka, Predicting porosity, permeability, and tortuosity of porous media from images by deep learning, Scientific reports 10 (1) (2020) 1–11.
- [6] J.-L. Wu, H. Xiao, E. Paterson, [Physics-informed machine learning approach for augmenting turbulence models: A case study](#), Phys. Rev. Fluids 3 (2018) 074602. [doi:10.1103/PhysRevFluids.3.074602](https://doi.org/10.1103/PhysRevFluids.3.074602).
URL <https://link.aps.org/doi/10.1103/PhysRevFluids.3.074602>
- [7] S. Otten, S. Caron, W. de Swart, M. van Beekveld, L. Hendriks, C. van Leeuwen, D. Podareanu, R. Ruiz de Austri, R. Verheyen, Event Generation and Statistical Sampling for Physics with Deep Generative Models and a Density Information Buffer, Nature Commun. 12 (1) (2021) 2985. [arXiv:1901.00875](#), [doi:10.1038/s41467-021-22616-z](https://doi.org/10.1038/s41467-021-22616-z).
- [8] T. J. Sejnowski, The Deep Learning Revolution, MIT Press, Cambridge, MA, 2018.
- [9] I. E. Lagaris, A. Likas, D. I. Fotiadis, Artificial neural networks for solving ordinary and partial differential equations, IEEE Transactions on Neural Networks 9 (5) (1998) 987–1000. [doi:10.1109/72.712178](https://doi.org/10.1109/72.712178).
- [10] I. Lagaris, A. Likas, D. Fotiadis, Artificial neural network methods in quantum mechanics, Computer Physics Communications 104 (1) (1997) 1 – 14.
- [11] M. Raissi, P. Perdikaris, G. E. Karniadakis, Physics informed deep learning (part i): Data-driven solutions of nonlinear partial differential equations, arXiv preprint [arXiv:1711.10561](https://arxiv.org/abs/1711.10561) (2017).
- [12] M. Raissi, P. Perdikaris, G. E. Karniadakis, Physics informed deep learning (part ii): Data-driven discovery of nonlinear partial differential equations, arXiv preprint [arXiv:1711.10566](https://arxiv.org/abs/1711.10566) (2017).
- [13] M. Raissi, P. Perdikaris, G. E. Karniadakis, Physics-informed neural networks: A deep learning framework for solving forward and inverse problems involving nonlinear partial differential equations, Journal of Computational Physics 378 (2019) 686–707.

- [14] S. Mishra, R. Molinaro, Physics informed neural networks for simulating radiative transfer, *Journal of Quantitative Spectroscopy and Radiative Transfer* 270 (2021) 107705. doi:10.1016/j.jqsrt.2021.107705.
- [15] S. Mishra, R. Molinaro, Estimates on the generalization error of physics informed neural networks (pinns) for approximating a class of inverse problems for pdes (2021). arXiv:2007.01138.
- [16] J. Sirignano, K. Spiliopoulos, Dgm: A deep learning algorithm for solving partial differential equations, *Journal of Computational Physics* 375 (2018) 1339–1364. doi:10.1016/j.jcp.2018.08.029. URL <http://dx.doi.org/10.1016/j.jcp.2018.08.029>
- [17] L. Lu, X. Meng, Z. Mao, G. E. Karniadakis, DeepXDE: A deep learning library for solving differential equations, *SIAM Review* 63 (1) (2021) 208–228. doi:10.1137/19m1274067. URL <https://doi.org/10.1137/19m1274067>
- [18] E. Haghghat, M. Raissi, A. Moure, H. Gomez, R. Juanes, A deep learning framework for solution and discovery in solid mechanics (2020). doi:10.48550/ARXIV.2003.02751. URL <https://arxiv.org/abs/2003.02751>
- [19] N. Thuerey, P. Holl, M. Mueller, P. Schnell, F. Trost, K. Um, *Physics-based Deep Learning*, WWW, 2021. URL <https://physicsbaseddeeplearning.org>
- [20] Z. Hao, J. Yao, C. Su, H. Su, Z. Wang, F. Lu, Z. Xia, Y. Zhang, S. Liu, L. Lu, J. Zhu, Pinnacle: A comprehensive benchmark of physics-informed neural networks for solving pdes (2023). arXiv:2306.08827.
- [21] S. Jiang, X. Li, Solving non-local fokker-planck equations by deep learning (2022). doi:10.48550/ARXIV.2206.03439. URL <https://arxiv.org/abs/2206.03439>
- [22] S. Subramanian, R. M. Kirby, M. W. Mahoney, A. Gholami, Adaptive self-supervision algorithms for physics-informed neural networks (2022). doi:10.48550/ARXIV.2207.04084. URL <https://arxiv.org/abs/2207.04084>
- [23] Z. Long, Y. Lu, X. Ma, B. Dong, Pde-net: Learning pdes from data (2017). doi:10.48550/ARXIV.1710.09668. URL <https://arxiv.org/abs/1710.09668>
- [24] S. Cuomo, V. S. di Cola, F. Giampaolo, G. Rozza, M. Raissi, F. Piccialli, Scientific machine learning through physics-informed neural networks: Where we are and what's next (2022). arXiv:2201.05624.
- [25] G. E. Karniadakis, I. G. Kevrekidis, L. Lu, P. Perdikaris, S. Wang, L. Yang, Physics-informed machine learning, *Nature Reviews Physics* 3 (6) (2021) 422–440.
- [26] S. A. Faroughi, N. Pawar, C. Fernandes, M. Raissi, S. Das, N. K. Kalantari, S. K. Mahjour, Physics-guided, physics-informed, and physics-encoded neural networks in scientific computing (2023). arXiv:2211.07377.
- [27] C. Meng, S. Seo, D. Cao, S. Griesemer, Y. Liu, When physics meets machine learning: A survey of physics-informed m (2022). doi:10.48550/ARXIV.2203.16797. URL <https://arxiv.org/abs/2203.16797>
- [28] Z. Hao, S. Liu, Y. Zhang, C. Ying, Y. Feng, H. Su, J. Zhu, Physics-informed machine learning: A survey on problems, methods and applications (2023). arXiv:2211.08064.
- [29] F. Rosenblatt, *Principles of Neurodynamics*, New York: Spartan, 1962. URL <http://www.dtic.mil/docs/citations/AD0256582>

- [30] J. Hertz, [Introduction To The Theory Of Neural Computation](#), CRC Press, 2018.
URL <https://books.google.pl/books?id=NwpQDwAAQBAJ>
- [31] I. Goodfellow, Y. Bengio, A. Courville, [Deep Learning](#), MIT Press, 2016,
<http://www.deeplearningbook.org>.
- [32] C. M., Bishop, [Neural Networks for Pattern Recognition](#), Oxford University Press, 1995.
- [33] G. D’Agostini, [Bayesian Reasoning in Data Analysis](#), World Scientific, 2003.
URL <http://www.worldscientific.com/worldscibooks/10.1142/5262>
- [34] H. Jeffreys, [Theory of Probability](#), Oxford University Press, 1961.
- [35] J. Gawlikowski, C. R. N. Tassi, M. Ali, J. Lee, M. Humt, J. Feng, A. Kruspe, R. Triebel, P. Jung, R. Roscher, M. Shahzad, W. Yang, R. Bamler, X. X. Zhu, [A survey of uncertainty in deep neural networks](#), *Artificial Intelligence Review* 56 (1) (2023) 1513–1589. doi:10.1007/s10462-023-10562-9.
URL <https://doi.org/10.1007/s10462-023-10562-9>
- [36] S. F. Gull, [Bayesian Inductive Inference and Maximum Entropy](#), Springer Netherlands, Dordrecht, 1988, pp. 53–74. doi:10.1007/978-94-009-3049-0_4.
URL https://doi.org/10.1007/978-94-009-3049-0_4
- [37] A. F. Psaros, X. Meng, Z. Zou, L. Guo, G. E. Karniadakis, [Uncertainty quantification in scientific machine learning: Methods, metrics, and comparisons](#), *Journal of Computational Physics* 477 (2023) 111902. doi:https://doi.org/10.1016/j.jcp.2022.111902.
URL <https://www.sciencedirect.com/science/article/pii/S0021999122009652>
- [38] Y. Zhu, N. Zabaras, [Bayesian deep convolutional encoder–decoder networks for surrogate modeling and uncertainty quantification](#), *Journal of Computational Physics* 366 (2018) 415–447. doi:10.1016/j.jcp.2018.04.018.
- [39] N. Geneva, N. Zabaras, [Modeling the dynamics of pde systems with physics-constrained deep auto-regressive networks](#), *Journal of Computational Physics* 403 (2020) 109056. doi:https://doi.org/10.1016/j.jcp.2019.109056.
URL <https://www.sciencedirect.com/science/article/pii/S0021999119307612>
- [40] A. Besginow, M. Lange-Hegermann, [Constraining gaussian processes to systems of linear ordinary differential equations](#) (2022). doi:10.48550/ARXIV.2208.12515.
URL <https://arxiv.org/abs/2208.12515>
- [41] C. Rasmussen, C. Williams, [Gaussian Processes for Machine Learning](#), Adaptive Computation and Machine Learning, MIT Press, Cambridge, MA, USA, 2006.
- [42] M. Raissi, P. Perdikaris, G. E. Karniadakis, [Machine learning of linear differential equations using gaussian processes](#), *Journal of Computational Physics* 348 (2017) 683 – 693. doi:https://doi.org/10.1016/j.jcp.2017.07.050.
- [43] M. Raissi, P. Perdikaris, G. E. Karniadakis, [Inferring solutions of differential equations using noisy multi-fidelity data](#), *Journal of Computational Physics* 335 (2017) 736–746.
- [44] R. M. Neal, [Bayesian learning for neural networks](#), Ph.D. thesis, Graduate Department of Computer Science in University of Toronto (1995).
- [45] L. Yang, X. Meng, G. E. Karniadakis, [B-pinns: Bayesian physics-informed neural networks for forward and inverse problems](#), *Journal of Computational Physics* 425 (2021) 109913. doi:10.1016/j.jcp.2020.109913.
URL <http://dx.doi.org/10.1016/j.jcp.2020.109913>
- [46] C. Bonneville, C. Earls, [Bayesian deep learning for partial differential equation parameter discovery with sparse and noisy data](#), *Journal of Computational Physics: X* 16 (2022) 100115.
- [47] K. More, T. Tripura, R. Nayek, S. Chakraborty, [A bayesian framework for learning governing partial differential equation from data](#) (2023). [arXiv:2306.04894](https://arxiv.org/abs/2306.04894).

- [48] L. Lu, P. Jin, G. Pang, Z. Zhang, G. E. Karniadakis, Learning nonlinear operators via deepnet based on the universal approximation theorem of operators, *Nature Machine Intelligence* 3 (3) (2021) 218–229. doi:[10.1038/s42256-021-00302-5](https://doi.org/10.1038/s42256-021-00302-5).
- [49] M. Magris, A. Iosifidis, *Bayesian learning for neural networks: an algorithmic survey* (2022). doi:[10.48550/ARXIV.2211.11865](https://doi.org/10.48550/ARXIV.2211.11865). URL <https://arxiv.org/abs/2211.11865>
- [50] D. MacKay, Bayesian methods for adaptive models, Ph.D. thesis, California Institute of Technology (1991).
- [51] D. J. C. MacKay, Bayesian interpolation, *Neural Computation* 4 (3) (1992) 415–447. arXiv:<https://doi.org/10.1162/neco.1992.4.3.415>, doi:[10.1162/neco.1992.4.3.415](https://doi.org/10.1162/neco.1992.4.3.415). URL <https://doi.org/10.1162/neco.1992.4.3.415>
- [52] D. J. C. MacKay, A practical bayesian framework for backpropagation networks, *Neural Computation* 4 (3) (1992) 448–472. arXiv:<https://doi.org/10.1162/neco.1992.4.3.448>, doi:[10.1162/neco.1992.4.3.448](https://doi.org/10.1162/neco.1992.4.3.448). URL <https://doi.org/10.1162/neco.1992.4.3.448>
- [53] S. F. Gull, *Developments in Maximum Entropy Data Analysis*, Springer Netherlands, Dordrecht, 1989, pp. 53–71. doi:[10.1007/978-94-015-7860-8_4](https://doi.org/10.1007/978-94-015-7860-8_4). URL https://doi.org/10.1007/978-94-015-7860-8_4
- [54] J. Skilling, *On Parameter Estimation and Quantified Maxent*, Springer Netherlands, Dordrecht, 1991, pp. 267–273. doi:[10.1007/978-94-011-3460-6_25](https://doi.org/10.1007/978-94-011-3460-6_25). URL https://doi.org/10.1007/978-94-011-3460-6_25
- [55] L. Alvarez-Ruso, K. M. Graczyk, E. Saul-Sala, Nucleon axial form factor from a Bayesian neural-network analysis of neutrino-scattering data, *Phys. Rev. C* 99 (2) (2019) 025204. arXiv:[1805.00905](https://arxiv.org/abs/1805.00905), doi:[10.1103/PhysRevC.99.025204](https://doi.org/10.1103/PhysRevC.99.025204).
- [56] K. M. Graczyk, C. Juszczak, Zemach moments of the proton from Bayesian inference, *Phys. Rev. C* 91 (4) (2015) 045205. doi:[10.1103/PhysRevC.91.045205](https://doi.org/10.1103/PhysRevC.91.045205).
- [57] K. M. Graczyk, C. Juszczak, Applications of Neural Networks in Hadron Physics, *J. Phys. G* 42 (3) (2015) 034019. arXiv:[1409.5244](https://arxiv.org/abs/1409.5244), doi:[10.1088/0954-3899/42/3/034019](https://doi.org/10.1088/0954-3899/42/3/034019).
- [58] K. M. Graczyk, Two-Photon Exchange Effect Studied with Neural Networks, *Phys. Rev. C* 84 (2011) 034314. arXiv:[1106.1204](https://arxiv.org/abs/1106.1204), doi:[10.1103/PhysRevC.84.034314](https://doi.org/10.1103/PhysRevC.84.034314).
- [59] A. Paszke, S. Gross, F. Massa, A. Lerer, J. Bradbury, G. Chanan, T. Killeen, Z. Lin, N. Gimelshein, L. Antiga, A. Desmaison, A. Kopf, E. Yang, Z. DeVito, M. Raison, A. Tejani, S. Chilamkurthy, B. Steiner, L. Fang, J. Bai, S. Chintala, Pytorch: An imperative style, high-performance deep learning library, in: *Advances in Neural Information Processing Systems* 32, Curran Associates, Inc., 2019, pp. 8024–8035.
- [60] O. Hennigh, S. Narasimhan, M. A. Nabian, A. Subramaniam, K. Tangsali, M. Rietmann, J. del Aguila Ferrandis, W. Byeon, Z. Fang, S. Choudhry, Nvidia simnetTM: an ai-accelerated multi-physics simulation framework (2020). arXiv:[2012.07938](https://arxiv.org/abs/2012.07938).
- [61] C. L. Wight, J. Zhao, Solving allen-cahn and cahn-hilliard equations using the adaptive physics informed neural networks (2020). arXiv:[2007.04542](https://arxiv.org/abs/2007.04542).
- [62] S. Wang, Y. Teng, P. Perdikaris, Understanding and mitigating gradient pathologies in physics-informed neural networks (2020). arXiv:[2001.04536](https://arxiv.org/abs/2001.04536).
- [63] S. Wang, X. Yu, P. Perdikaris, When and why pinns fail to train: A neural tangent kernel perspective (2020). arXiv:[2007.14527](https://arxiv.org/abs/2007.14527).
- [64] L. McClenny, U. Braga-Neto, Self-adaptive physics-informed neural networks using a soft attention mechanism (2022). arXiv:[2009.04544](https://arxiv.org/abs/2009.04544).

- [65] G. Cybenko, [Approximation by superpositions of a sigmoidal function](#), *Math Control, Signal* 2 (4) (1989) 303. doi:[10.1007/BF02551274](https://doi.org/10.1007/BF02551274).
URL <http://dx.doi.org/10.1007/BF02551274>
- [66] K. Hornik, M. Stinchcombe, W. Halbert, Multilayer feedforward networks are universal approximators, *Neural Networks* 2 (1989) 359. doi:<http://www.sciencedirect.com/science/article/pii/0893608089900208>.
- [67] K.-I. Funahashi, [On the approximate realization of continuous mappings by neural networks](#), *Neural Networks* 2 (3) (1989) 183–192. doi:[https://doi.org/10.1016/0893-6080\(89\)90003-8](https://doi.org/10.1016/0893-6080(89)90003-8).
URL <http://www.sciencedirect.com/science/article/pii/0893608089900038>
- [68] S. Geman, E. Bienenstock, R. Doursat, [Neural networks and the bias/variance dilemma](#), *Neural Computation* 4 (1) (1992) 1–58. arXiv:<https://doi.org/10.1162/neco.1992.4.1.1>, doi:[10.1162/neco.1992.4.1.1](https://doi.org/10.1162/neco.1992.4.1.1).
URL <https://doi.org/10.1162/neco.1992.4.1.1>
- [69] R. Hanson, J. Stutz, P. Cheeseman, Bayesian classification theory, Tech. Rep. Technical Report F[A-90-12-7-01, NASA (05 1991).
- [70] J. O. Berger, J. O. Berger, *Statistical decision theory and Bayesian analysis*, Springer-Verlag, New York, 1985.
- [71] A. M. Chen, H.-m. Lu, R. Hecht-Nielsen, [On the Geometry of Feedforward Neural Network Error Surfaces](#), *Neural Computation* 5 (6) (1993) 910–927. arXiv:<https://direct.mit.edu/neco/article-pdf/5/6/910/812656/neco.1993.5.6.910.pdf>, doi:[10.1162/neco.1993.5.6.910](https://doi.org/10.1162/neco.1993.5.6.910).
- [72] H. H. Thodberg, [Ace of bayes : Application of neural](#), 1993.
URL <https://api.semanticscholar.org/CorpusID:15593225>
- [73] D. P. Kingma, J. Ba, Adam: A method for stochastic optimization (2017). arXiv:[1412.6980](https://arxiv.org/abs/1412.6980).
- [74] Y. Zhang, P. Khanduri, I. Tsaknakis, Y. Yao, M. Hong, S. Liu, [An introduction to bi-level optimization: Foundations and applications in signal processing and machine learning](#) (2023). arXiv:[2308.00788](https://arxiv.org/abs/2308.00788).
- [75] S. Brooks, A. Gelman, G. Jones, X.-L. Meng, [Handbook of Markov Chain Monte Carlo](#), Chapman and Hall/CRC, 2011. doi:[10.1201/b10905](https://doi.org/10.1201/b10905).
URL <http://dx.doi.org/10.1201/b10905>